Forest Condition Monitoring Using Very-High-Resolution Satellite Imagery in a Remote Mountain Watershed in Nepal

Authors: Uddin, Kabir, Gilani, Hammad, Murthy, M. S. R., Kotru, Rajan, and Qamer, Faisal Mueen

Source: Mountain Research and Development, 35(3) : 264-277

Published By: International Mountain Society

URL: https://doi.org/10.1659/MRD-JOURNAL-D-14-00074.1

Mountain Research and Development (MRD)
An international, peer-reviewed open access journal
published by the International Mountain Society (IMS)
www.mrd-journal.org

MountainResearch
Systems knowledge

Forest Condition Monitoring Using Very-High-Resolution Satellite Imagery in a Remote Mountain Watershed in Nepal

Kabir Uddin, Hammad Gilani, M. S. R. Murthy, Rajan Kotru, and Faisal Mueen Qamer*
** Corresponding author: Kabir.Uddin@icimod.org*
International Centre for Integrated Mountain Development, GPO Box 3226, Kathmandu, Nepal

Satellite imagery has proven extremely useful for repetitive timeline-based data collection, because it offers a synoptic view and enables fast processing of large quantities of data. The changes in tree crown number and land cover in a very remote watershed (area 1305 ha) in Nepal were analyzed using a QuickBird image from 2006 and an IKONOS image from 2011. A geographic object-based image analysis (GEOBIA) was carried out using the region-growing technique for tree crown detection, delineation, and change assessment, and a multiresolution technique was used for land cover mapping and change analysis. The coefficient of determination for tree crown detection and delineation was 0.97 for QuickBird and 0.99 for IKONOS, calculated using a line-intercept transect method with 10 randomly selected windows (1×1 ha). The number of tree crowns decreased from 47,121 in 2006 to 41,689 in 2011, a loss of approximately 90 trees per month on average; the area of needle-leaved forest was reduced by 140 ha (23%) over the same period. Analysis of widely available very-high-resolution satellite images using GEOBIA techniques offers a cost-effective method for detecting changes in tree crown number and land cover in remote mountain valleys; the results provide the information needed to support improved local-level planning and forest management in such areas.

Keywords: *Satellite imagery; geographic object-based image analysis (GEOBIA); tree crown detection; land cover mapping; GIS; Nepal.*

Peer-reviewed: *March 2015* ***Accepted:*** *June 2015*

Introduction

The importance of forests and the problems posed by deforestation and forest degradation have been discussed widely in recent years (Hansen et al 2003; FAO 2011; Lambin and Meyfroidt 2011). In the Hindu Kush–Himalayan (HKH) region, forests play an essential role in maintaining the health of the mountain ecosystem and provide mountain people with fuel, food, construction materials, animal feed, and a source of income. They also play an essential role in the hydrological cycle and contribute to reduction of disaster risk (Smith 2013). While forest loss contributes to climate change, forests can also play an important role in mitigation and adaptation through protection and management to increase carbon sequestration (Karki et al 2014).

Despite the widespread recognition of the importance of forests, deforestation and forest degradation continue to be a challenge in the HKH region as elsewhere and are likely to be compounded in future years by climate change. Planning and management to slow or reverse forest loss requires detailed information on forest status and change over time; so does assessment of the impacts of any interventions. But there is less precise information available in the region on the extent of current forest cover or deforestation rates, particularly the detailed information required for planning and assessing local-level activities. It is especially challenging to gather detailed information on forest extent at ground level in the remote and poorly accessible valleys of the HKH, and even more so to repeat measurements over time. A different approach is required to gather such information.

Satellite images are extremely useful for repetitive timeline-based data collection across large areas, because they offer a synoptic view and the possibility of fast processing of large quantities of data. The high correlation between the spectral bands of satellite images and vegetation parameters make this method the primary source for large-area monitoring of land cover characteristics, especially in remote and rough terrain (Baccini et al 2004; Lu 2006; Uddin et al 2015). It has major advantages over in situ measurements in enabling cost-effective and continuous monitoring of natural resources. More recently, very-high-resolution (VHR) satellite images such as Cartosat, GeoEye, IKONOS, QuickBird, SPOT-5, and WorldView have become available that can be used for detailed monitoring, for

example, to extract forest structures and model individual tree parameters (Gibbs et al 2007; Leboeuf et al 2007). Using VHR satellite images is much less costly than carrying out exhaustive ground measurements and can provide extensive, accurate, and timely monitoring and measurements (Immitzer et al 2012). Geographic object-based image analysis (GEOBIA) provides an opportunity to improve the details in land cover (LC) and land use (LU) maps and assessments of forest parameters (eg tree crown detection and delineation, tree species classification, and identification and monitoring of degraded forest land) (Erikson 2004; Erikson and Olofsson 2005; Ke and Quackenbush 2011; Immitzer et al 2012; Pu and Landry 2012).

A number of algorithms are available for satellite image classification, both pixel- and object-based. Image segmentation techniques were developed in the 1980s but were used to only a small extent in geospatial applications (Blaschke 2010). Following recent rapid development, object- or segmentation-based image classification algorithms now provide much faster and more accurate results than conventional pixel-based algorithms (Stathakis and Vasilakos 2006; Thessler et al 2008; Knorn et al 2009; Blaschke 2010; Quintano and Cuesta 2010). Various GEOBIA techniques have been used for tree crown detection and delineation, including valley following (Ke and Quackenbush 2011), region growing (Culvenor 2002; Ke and Quackenbush 2008), watershed transformation (Wang et al 2004), multiresolution segmentation (Kim et al 2009), wavelet segmentation (Coillie et al 2008), and multiscale object-specific segmentation (Hay et al 2005). Larsen et al (2011) compared 6 different algorithms for tree crown detection under a variety of forest conditions: local maxima detection, valley following, template matching, scale-space theory, Markov random fields, and marked point processes. Detection and delineation of tree crowns can be used to model tree structural variables (eg stem diameter, height, and biomass), which are useful in forest inventory and evaluation of growth performance (Culvenor 2002). Now a number of researchers are starting to use segmentation techniques integrated with active (Light Detection and Ranging [LiDAR]) and passive (multispectral) remote sensing data sets to obtain more accurate and precise results in forested areas (Erdody and Moskal 2010; Kim et al 2010; Mbaabu et al 2014; Thapa et al 2014).

Uniform or consistent data sets in a defined timeframe are essential for monitoring of natural systems that may be influenced by human activities or changes in climate. LCLU maps show the overall changes in existing land features, but VHR satellite images and algorithms are required to understand the dynamics of specific features such as trees within and outside of forested areas. Bai et al (2005) used IKONOS (2006) and WorldView-2 (2011) images for GEOBIA-based quantification and comparative analysis of urban tree species in the city of Tampa, Florida, USA. Ke and Quackenbush (2011) described 3 methods for evaluation and ensuring accuracy of detected and delineated tree crowns through satellite images: (1) how well the delineated crowns represent the position of reference crowns, (2) how well the delineated crown size represents the actual size of reference crowns, and (3) how well the results represent the forest stand properties. According to Ke and Quackenbush (2011), there is no well-established method for accurate assessment of detected and delineated tree crowns, but the most commonly used method is to compare the total number of detected trees against reference tree counts at plot level (Culvenor 2002; Ke and Quackenbush 2011). However, one-to-one (canopy-to-canopy) assessment is very challenging for tree crown change due to both systematic and nonsystematic errors that occur during the acquisition of satellite images over different periods (Potere 2008).

Understanding the detailed dynamics of LCLU in a small area depends greatly on the spatial resolution of the satellite imagery, because spatial resolution affects image classification results. Following the advent of VHR satellite data (resolution < 5 m), it is now possible to derive detailed LCLU information at a level sufficient to support watershed-level planning. Pu et al (2011) identified significant improvements in classification accuracy using GEOBIA—compared to pixel-based methods—using IKONOS imagery. Similarly, Mathieu et al (2007) used IKONOS imagery and object-based classification to identify 20 LCLU classes for the city of Dunedin, New Zealand, with results similar to those of Pu et al (2011).

Real-time accuracy assessment based on field data is very important for identification, verification, and use of remote-sensing-derived products, although several studies have had to depend on existing field or secondary information due to limitations of resources and time (Stehman and Czaplewski 1998; Foody 2002). Various sources such as coordinates recorded through global positioning system (GPS) receivers, field photographs, topographic sheets, and interviews can be used for accuracy assessment and validation of derived products.

The main objective of the present study was to assess the feasibility of using GEOBIA techniques with VHR satellite images (QuickBird and IKONOS) to detect, delineate, and count tree crowns, prepare LC maps, and detect changes over time, in a cost-effective manner in remote and otherwise poorly accessible mountain valleys of Nepal. The Lorpa watershed in Jumla district was used as an example, with the specific objectives of detecting and delineating tree crowns size in 2006 and 2011, preparing LC maps, and using the results to assess LC change over this 5-year period.

Material and methods

Study area

Jumla is a mountain district located in the Mid-western Development Region of Nepal. The area is historically significant and is considered to be the center of origin of the Nepali language. It is also known for its biodiversity and spectacular scenery. It is one of the least developed districts of Nepal, ranking 68th out of 75 (National Population and Housing Census 2012). The temperature ranges from +33°C in summer to −15°C in winter; average annual rainfall is approximately 800 mm, of which about 450 mm falls between July and September. There is a marked variation in elevation, and the climate ranges from cold temperate at lower elevations (<3000 masl), through alpine at middle elevations (3000–4500 masl), to tundra at the highest elevations (> 4500 masl). The study was conducted in the Lorpa watershed in Jumla district (Figure 1). The watershed's center point lies at 82°15′36″E and 29°20′24″N. It has a total area of 13.05 km^2, elevation range from 2497 to 4078 masl, and range of slope from 0.5° to 77°. The watershed includes parts of the Dillichaur and Patmara village development committee areas and has 2 main villages: Mathillo Lorpa and Tallo Lorpa. Agriculture is the main source of livelihood, with some additional income from wage labor and small business. There are large areas of forest, some rangeland, and a small area of agricultural land in the flatter part of the lower catchment.

Remote sensing data and preprocessing

A QuickBird satellite image acquired on 18 November 2006 and an IKONOS satellite image acquired on 24 October 2011 were used for change detection. The QuickBird panchromatic sensor collects a single band of data in the spectral range of 405–1053 nm at 0.5 m resolution, and the QuickBird multispectral sensor collects 4 bands of data in the spectral bands of 450–545 nm (blue), 466–620 nm (green), 590–710 nm (red), and 715–918 nm (near-infrared) at 2 m resolution. The IKONOS panchromatic sensor collects a single band of data in the spectral range of 760–850 nm at 1 m resolution, and its multispectral sensor collects 4 bands of data in the spectral bands of 445–516 nm (blue), 506–595 nm (green), 632–698 nm (red), and 757–853 nm (near infrared) at 4 m spatial resolution. The shuttle radar topography mission (SRTM) digital elevation model (DEM), with add-on products such as slope and aspect, was used for topographic information. Base layers (like settlements, roads, and contours) in vector format (shapefiles) were used both as baseline information for the maps and for LC extraction. GPS coordinates and field photographs were used as ancillary information for the identification of LC features on the satellite images.

The IKONOS and QuickBird images were orthorectified individually band by band using rational polynomial coefficient files along a horizontal 90 m (3 arc second) SRTM DEM by applying the cubic convolution method in zone 44 of the UTM (universal transverse Mercator) coordinate system. WGS (world geodetic system) 84 was chosen as datum and spheroid. Although there is a large difference between the resolution of the VHR satellite images and that of the SRTM DEM, the STRM has been found to be better than any other DEM available in the public domain (Suwandana et al 2012). The accuracy of the rectified images was evaluated using GPS readings recorded on the ground.

The multispectral imagery's resolution was improved through a resolution merge process with the help of a higher-spatial-resolution panchromatic band for better spatial visualization and further processing. However, positional differences were observed after the images were overlaid. Sensor azimuth angles with 47.37° deference were observed to be 210° and 162.63° for IKONOS and QuickBird images, respectively. To overcome this positional problem, the multispectral IKONOS image was further rectified. In the 2 data sets, 26 ground control points were selected; they showed an overall root mean square error of 1.2 m for panchromatic images and 1.5 m for multispectral images. Prior to segmentation, low-pass median filters were applied to minimize oversegmentation and smooth the appearance (Platt and Schoennagel 2009). Convolution 3×3 low-pass filters were used to reduce local variation, remove noise, enhance tree features, and improve the quality of the analyzed satellite images.

Tree crown detection, delineation, and change analysis

Tree crowns were delineated using QuickBird and IKONOS images applying the region-growing technique in eCognition Developer. Prior to segmentation, a low-pass filter was applied to smooth the image to avoid oversegmentation (Platt and Schoennagel 2009). This filter produces more homogenous image segments and may reduce the amount of convolutions in the final segmented polygons (Mora et al 2010). In this study, we developed a local maxima algorithm to identify tree tops. From the tree top, the segments were grown to identify tree crown area (Figure 2). The first step in region-growing was to create image objects using multiresolution segmentation. Second, we identified the brightest pixels, which were then used as seed pixels (tree tops). Regions were "grown" from the seed pixels to the local minima, resulting in homogeneous objects based on predefined homogeneity criteria (Erikson 2003; Shih and Cheng 2005; Cui et al 2008).

The tree crown maps provided information on the occurrence of trees in both forest and nonforest categories and enabled assessment of changes over time in the overall tree count and the number of trees in different crown density categories. A 1-ha homogenous grid was created for the entire study area to compare the

FIGURE 1 Location of the Lorpa watershed in Jumla district, Nepal. (Map by the authors)

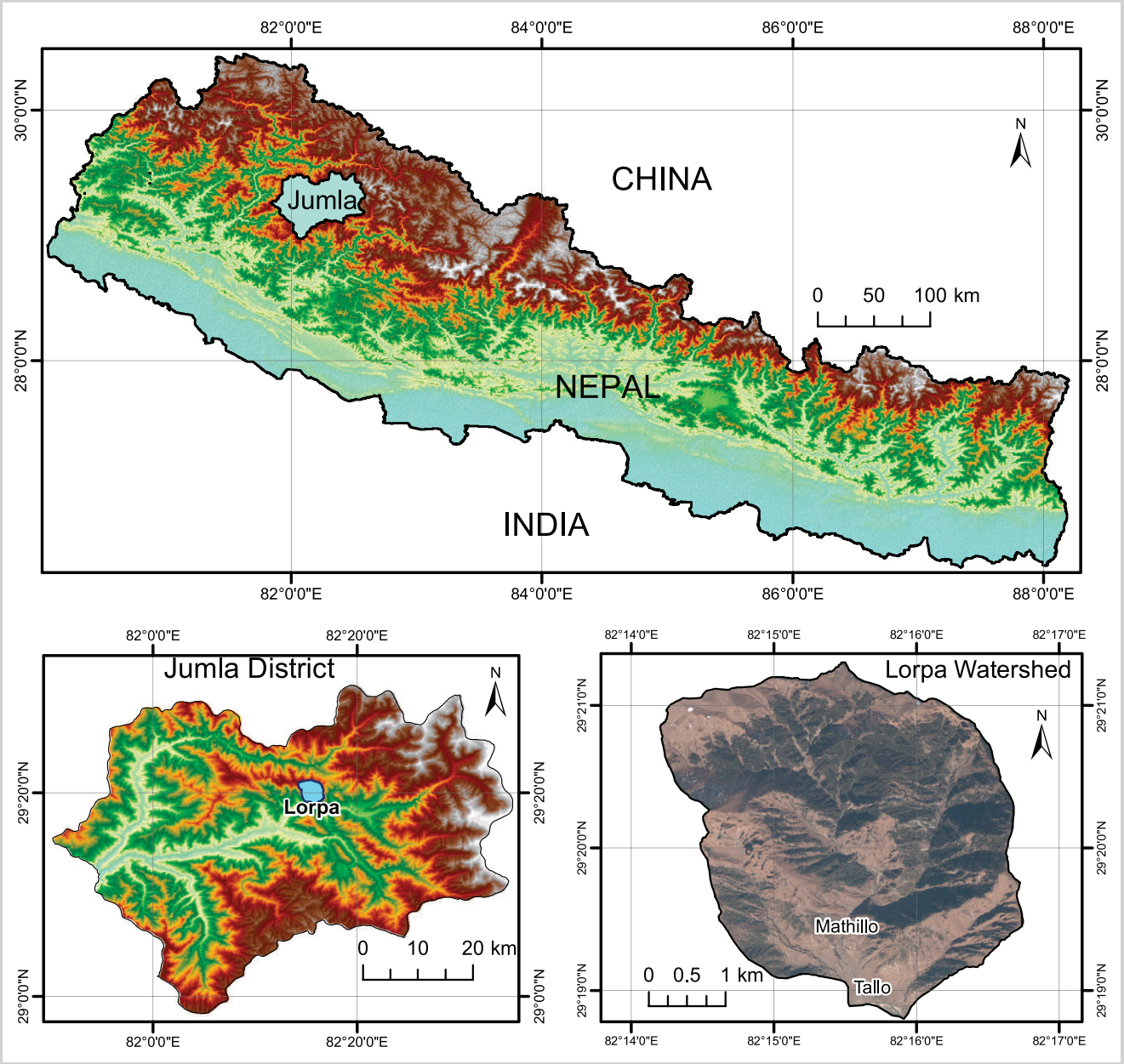

number and size of tree crowns in ArcGIS. Finally, the number of crowns in 2006 and 2011 were counted and compared to identify changes.

Land cover classification and change analysis

For the QuickBird and IKONOS image classification, the GEOBIA technique was used following Bajracharya et al (2010) and an algorithm developed by Uddin et al (2015). The image segments thus developed were used as the basic unit of classification, and each segment was attributed to a particular LC class using a set of defined rules based on information from spectral bands, indices, shape, color, and contextual parameters. The rules were developed for each QuickBird and IKONOS scene to overcome the inherent variability that arises in reflectance values across scenes because of the different times of acquisition. A minimum of 5 reference segments were selected for each class using field information to develop the rules. The image metrics for a given class were chosen according to their relative importance and potential to delineate the class. The thresholds for each metric were fixed iteratively by visual analysis using 2-dimensional feature plots and

http://dx.doi.org/10.1659/MRD-JOURNAL-D-14-00074.1

FIGURE 2 Image analysis to delineate tree crowns: (A) satellite image; (B) local maxima/tree tops; (C) distance from tree tops; (D) tree crowns.

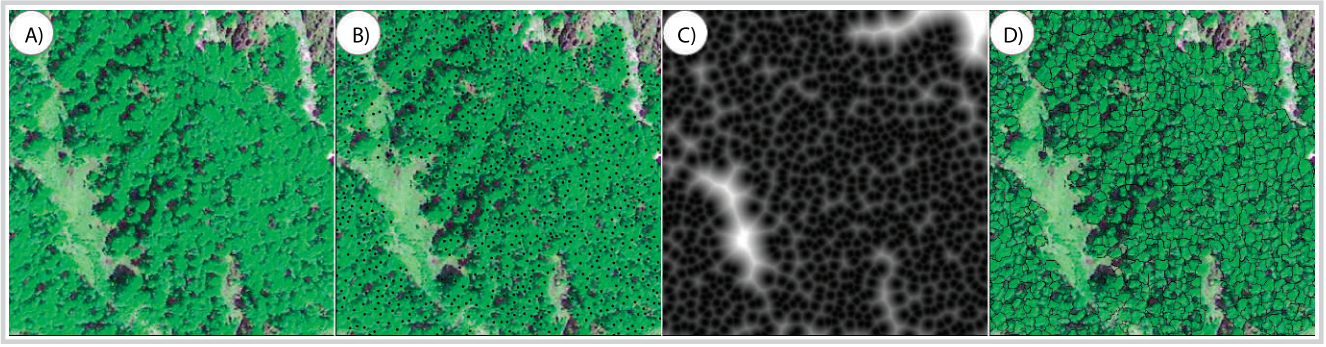

validating with reference segments. The rules with 90% class separability (based on reference segments) were chosen for application over the entire scene. After ascertaining the class separation using the segment-based approach, classification was performed to obtain an LC classification of both scenes.

LC detection using satellite data is an attempt to identify natural and human impacts on earth (Bajracharya et al 2010; Qamer et al 2012). The LC maps from 2006 and 2011 were evaluated and the area of the different classes compared. A change matrix and cross-tabulated values were used to identify changes over the 5 years. For the change matrix, the original 10 classes (Table 1) were reduced to 8, with the "built-up," "barren," and "river" classes subsumed into "other." In a change matrix, diagonal values show the stability of a class, while commission and omission values indicate a shift in area or percentage between classes (Olofsson et al 2013). Using the change matrix, "gross change, forest to nonforest," "gross change, nonforest to forest," and "net change" were extracted at watershed level. Changes in LC between 2006 and 2011 were also identified visually.

Accuracy assessment

Ten 1-ha windows were selected randomly for accuracy assessment of the detected and delineated tree crowns in the 2006 QuickBird and 2011 IKONOS images. Tree crowns were delineated manually and counted in each window using an image interpretation technique and then delineated and counted automatically in the same windows using the region-growing technique (Tiede et al 2006; Tiede et al 2007). A linear regression line was plotted between the 2 values and the coefficient of determination calculated.

Field verification was carried out at 60 randomly selected points in the watershed to assess the accuracy of the 2006 and 2011 LC maps. The geographic coordinates of the points were recorded together with the identified

TABLE 1 Land cover classes in the study area.

Land cover class	Description
Agricultural land	Agricultural areas currently cultivated, harvested, or fallow
Closed needle-leaved forest	Areas covered with trees with ≥40% canopy cover
Open needle-leaved forest	Areas covered with trees with 10 <40% canopy cover
Closed shrubland	Areas covered with shrubs with >40% canopy cover
Open shrubland	Areas covered with shrubs with 10 <40% canopy cover
Closed grassland	Land with closed grassland and scattered shrubs
Open grassland	Land with open grassland scattered shrubs
Built-up area	Human settlements
Barren area	Other areas with no vegetation cover
River/riverbed	Perennial rivers and rivers with little or no water[a)]

[a)]There are no other water bodies in this watershed.

http://dx.doi.org/10.1659/MRD-JOURNAL-D-14-00074.1

FIGURE 3 Tree crown maps: (A) sample area from QuickBird 2006; (B) sample area from IKONOS 2011.

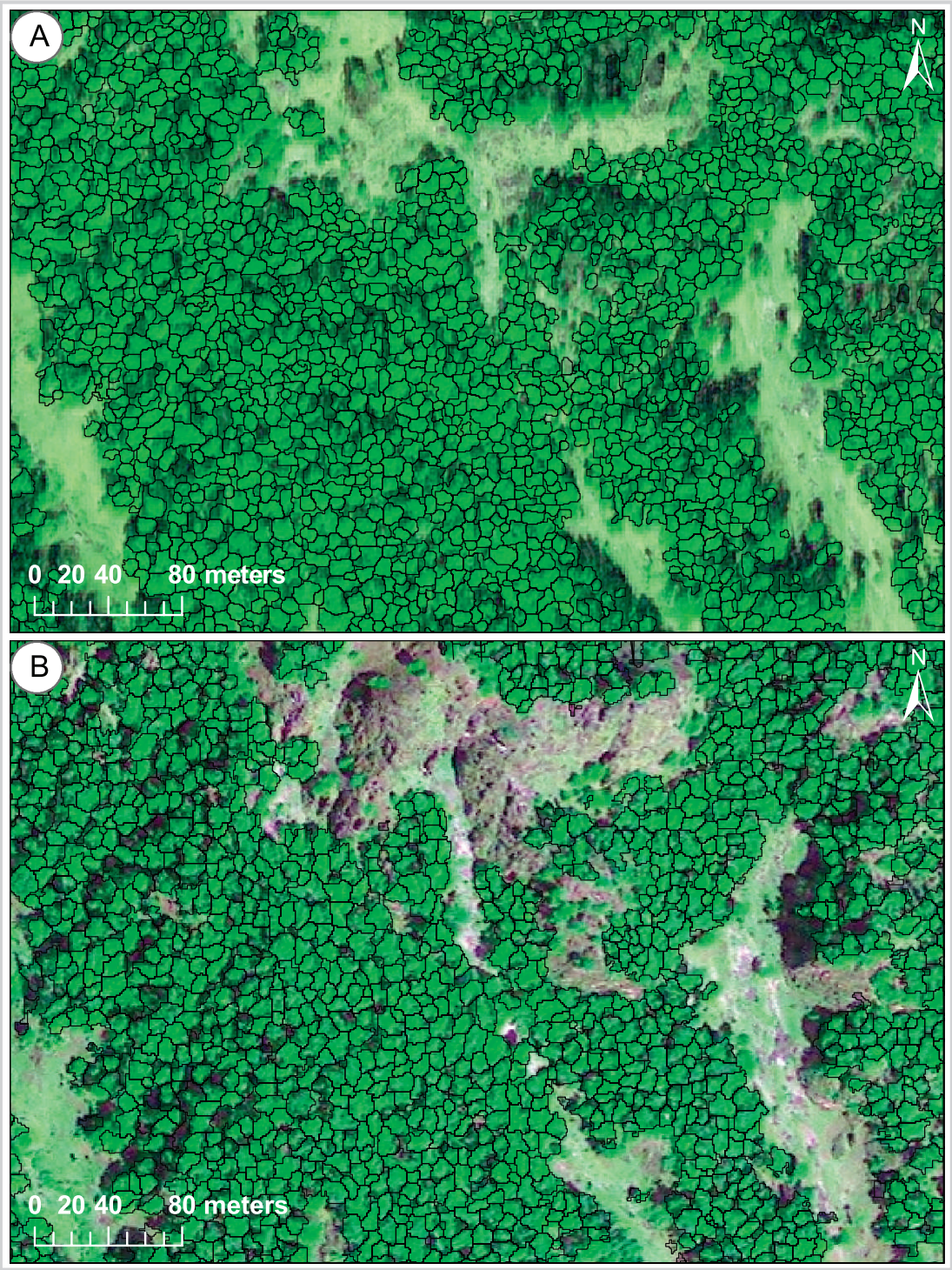

LC category. The sample points covered a range of locations and features but were insufficient to fully assess the LC accuracy. Thus, 80 additional randomly distributed points were selected in the raw IKONOS satellite image, the LC features identified by visual interpretation, and the results compared with the class on the LC map, giving a total of 140 points for the accuracy assessment.

http://dx.doi.org/10.1659/MRD-JOURNAL-D-14-00074.1

FIGURE 4 Number of tree crowns per hectare in a sample location, using: (A) QuickBird 2006; (B) IKONOS 2011.

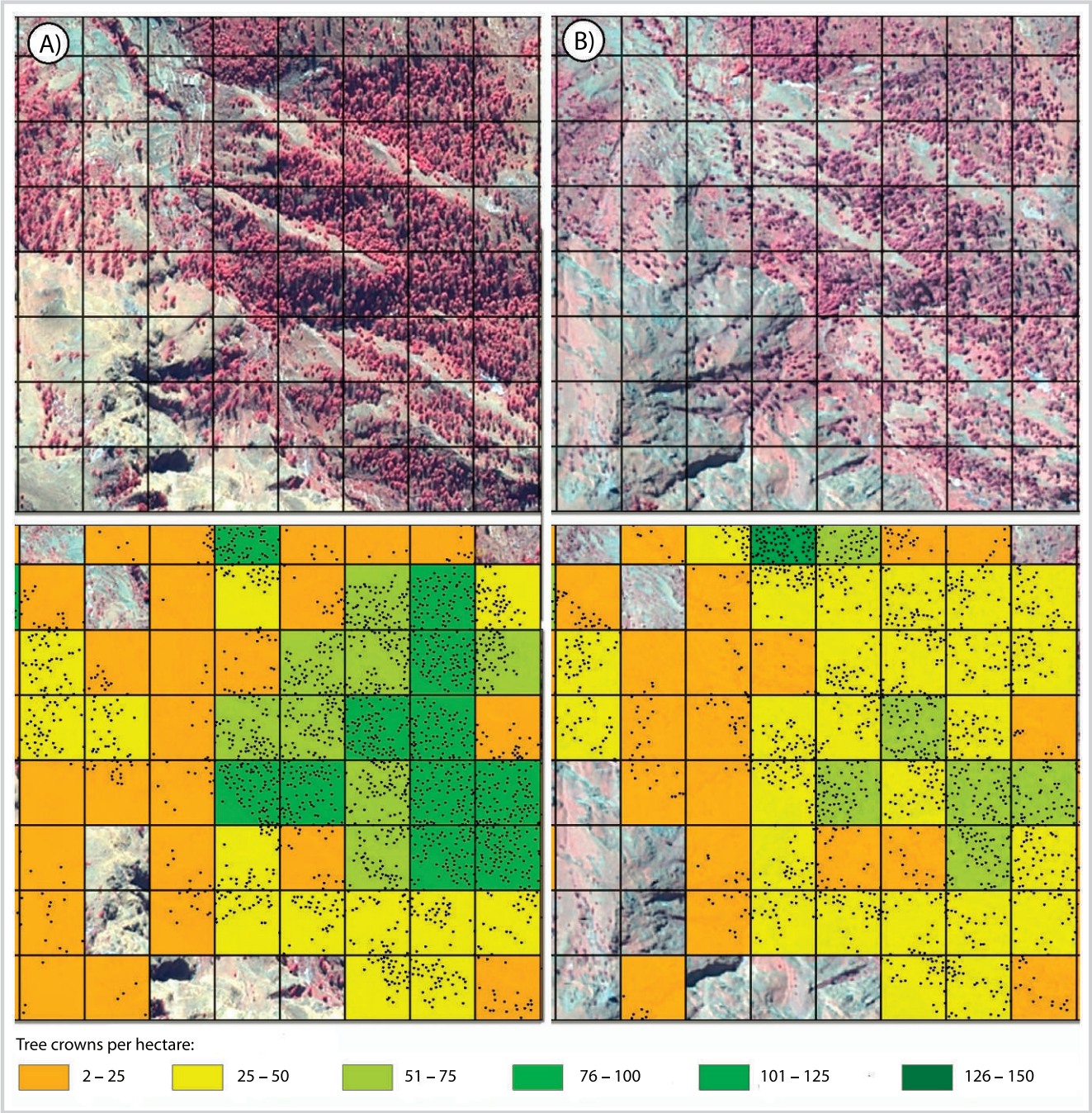

Results

A total of 47,121 tree crowns were detected and delineated in the 2006 QuickBird image, but only 41,689 in the 2011 IKONOS image, amounting to a reduction of 5,432 or 12%, equivalent to a loss of approximately 90 trees per month. The reduction was particularly strong in the southwestern part of the watershed, where the 2 settlements are located. Figure 3 shows 2 typical tree crown maps of the same central area of the watershed, generated in 2006 and 2011 using the region-growing technique for tree crown detection and delineation.

The tree crowns were classified into 5 size categories based on individual tree crown area. The number of

http://dx.doi.org/10.1659/MRD-JOURNAL-D-14-00074.1

FIGURE 5 Maps of the Lorpa watershed showing land cover in 2006 and 2011 (A) and land cover change from 2006 to 2011 (B). (Maps by the authors)

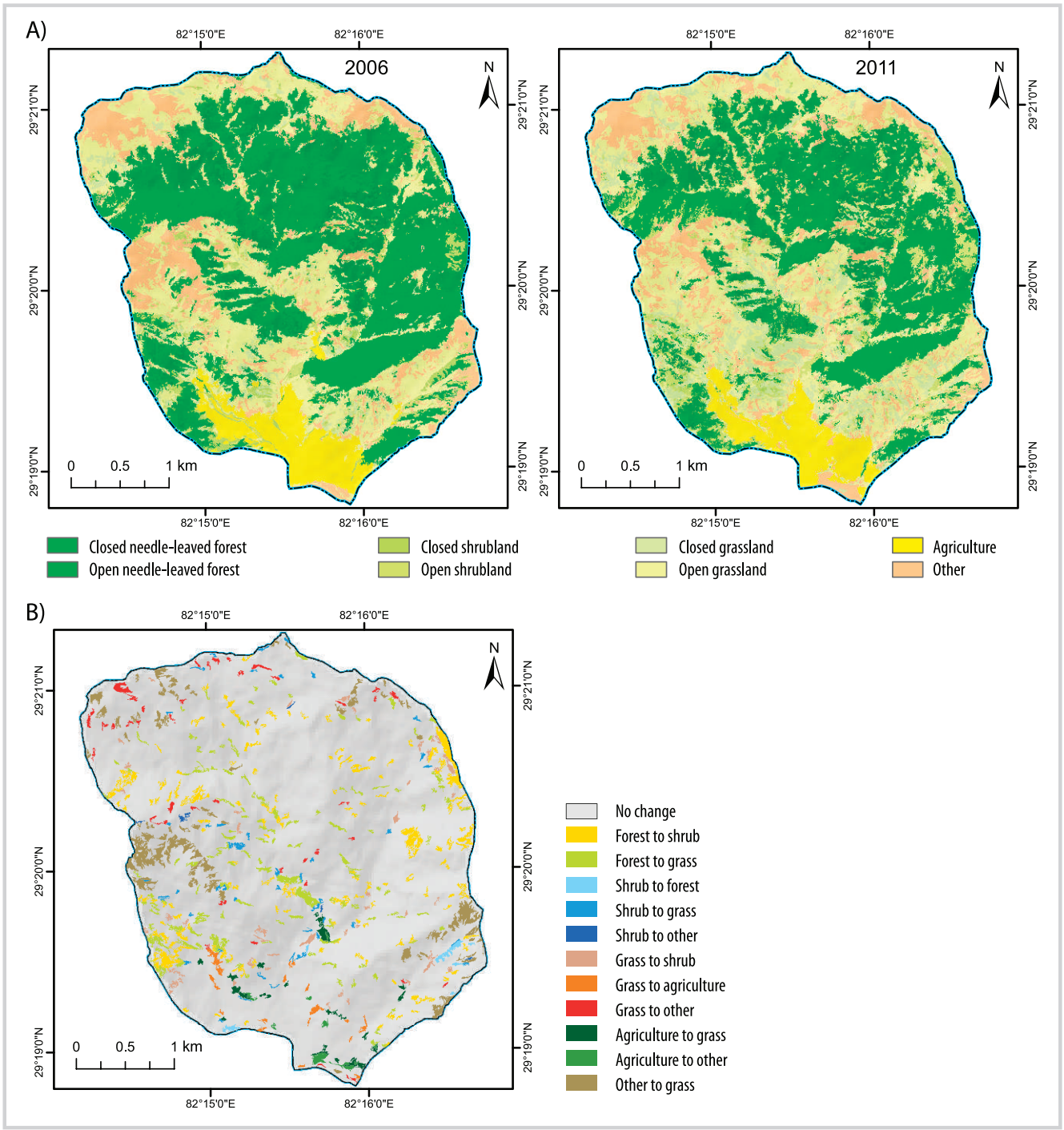

tree crowns in each category in 2006 and 2011 is shown in Figure 4. The number of trees in all tree crown categories decreased between 2006 and 2011, with the exception of trees with a crown area of 25–50 m^2, which showed a marked increase, and trees with a crown area of 50–75 m^2, which remained almost the same; the greatest loss was observed in trees with the greatest crown area, >100 m^2 (*Supplemental material*, Figure S1: http://dx.doi.org/10.1659/MRD-JOURNAL-D-14-00074.S1).

The validation analysis showed that the technique had a very high level of accuracy; the coefficient of

determination between algorithm delineated and visually recognized and delineated tree crowns was 0.97 for QuickBird and 0.99 for IKONOS (*Supplemental material*, Figure S2: http://dx.doi.org/10.1659/MRD-JOURNAL-D-14-00074.S1).

Forest was the largest LC class in the watershed (Figure 5). The total area of needle-leaved forest decreased from 634 ha in 2006 (48.59% of the total land area) to 493 ha in 2011 (37.78% of the total land area) (Table 2). The total area of the second largest class, grassland, increased from 347 ha in 2006 to 436 ha in 2011, an increase of 6.83% of the original cover. The proportion of the total area covered by closed shrubland decreased by 4.52% between 2006 and 2011, while that covered by open shrubland increased by 6%, an overall increase of 5%, and an 80% increase in the original shrubland area. The proportion of agricultural land decreased slightly from 79 to 72 ha. There was no change in the total area of the settlement, barren land, and river/riverbed classes. In terms of changes, 166 ha changed from forest to nonforest and 26 ha from nonforest to forest, a net loss of forest of 140 ha (Figure 5). These results show extensive deforestation and forest degradation in the watershed during the 5 years covered by the study, with an average loss of 90 trees per month, or more than 4% of the cover per year.

The accuracy of the LC maps was assessed by comparing the LC class in the map with the LC class identified by manual assessment at 140 randomly distributed points (60 on the ground and 80 in the IKONOS image). The accuracy assessments are shown in Tables 3 and 4.

Discussion

This study was conducted in the small Lorpa watershed in Jumla district, Nepal, to assess and monitor natural resources, especially forest. The results indicate that tree cutting remains an ongoing problem in the watershed, especially cutting of the larger, mature trees. During the late 1980s, marketing problems and poor crop returns forced many farmers to cut down their mature trees (Tiwari 2010). According to our remote sensing analysis, some of the loss is compensated by increased numbers of young trees growing to a canopy size of 25–50 m^2 and regeneration of trees with a canopy size of <25 m. But regeneration was slightly lower in 2011 than in 2006, and the new growth did not compensate for loss of mature trees in terms of either number or area.

We used the region-growing technique for the detection and delineation of tree crowns from commercially available QuickBird 2006 and IKONOS 2011 images. A number of authors have confirmed that this technique provides higher accuracy than other algorithms. Cui et al (2008) noted that it is a robust method that can extract objects and boundaries smoothly. Erikson and Olofsson (2005) compared the application of 3 different tree crown delineation methods—template matching (Olofsson et al 2006), 2 region-growing algorithms based on fuzzy rules (Brandtberg 2002), and Brownian motion—and found that all 3 approaches showed an overall accuracy of around 80%. Ke and Quackenbush (2008) concluded that region growing was more accurate than other methods in a study comparing region growing and valley following, as did Erikson and Olofsson (2005), who compared region growing with other algorithms. Similarly, Hussin et al (2014), who compared the region-growing and valley-following approaches, concluded that the region-growing approach showed better delineation than the valley-following approach because region growing is more flexible in detecting tree crowns of different sizes, since it uses both local maxima and local minima. Culvenor (2002) also found that the total number of trees delineated in a needle-leaved forest using a region-growing technique was almost identical to the number of trees counted on the ground (Ke and Quackenbush 2011). The greater accuracy of the technique may be because the method allows different parameters (eg crown width and roundness) to be set.

Other authors have also used commercially available VHR satellite data to obtain information on such factors as tree numbers (Mathieu et al 2007; Zhou et al 2013), tree species (Erikson 2004; Immitzer et al 2012; Latif et al 2012), and forest canopy structure and health (Pouliot et al 2002; Lévesque and King 2003; Chubey 2006) in other parts of the world for use in forest management. GEOBIA techniques have generally been found to be much more suitable for the detection and delineation of tree crowns and evaluation of LCLU than pixel-based classification algorithms (Zhou et al 2013) and were therefore the method of choice in the present study, as exemplified above. Species-level classification could be performed, but in this study, 10 optimum LC classes were mapped and compared without compromising the accuracy of each class. During digital image classification, the analyst incorporated field experience.

The change in forest cover could be seen clearly in the satellite images (*Supplemental material*, Figure S3: http://dx.doi.org/10.1659/MRD-JOURNAL-D-14-00074.S1). Overall in Nepal, changes in forest policy have led to immense progress in community-based conservation and restoration of forests (Agrawal and Chhatre 2006; Niraula et al 2013). As elsewhere in the HKH region, local livelihoods in the Lorpa watershed are closely linked to forests and scrub vegetation. Villagers, who need trees for fuel and for construction, have a vested interest in maintaining forest but are also dependent on it (Gilmour 1990). The study area is dominated by rangeland, with only small areas of forest

TABLE 2 Land cover in hectares, 2006 (rows) and 2011 (columns).

Land cover	Agriculture	Closed needle-leaved forest	Open needle-leaved forest	Closed shrubland	Open shrubland	Closed grassland	Open grassland	Other	Total (2006)	% of total area
Agriculture	67.0	0.0	0.0	0.0	1.0	3.0	6.0	5.0	**82**	6.44
Closed needle-leaved forest	0.0	264.5	9.0	7.0	21.0	5.0	13.0	2.0	**322**	24.60
Open needle-leaved forest	0.0	11.3	191.7	1.0	48.0	15.0	36.0	9.0	**312**	23.99
Closed shrubland	2.0	0.4	3.7	2.0	10.6	3.0	8.0	3.0	**33**	2.61
Open shrubland	1.0	0.0	3.0	3.0	11.0	6.0	16.0	3.0	**43**	3.22
Closed grassland	0.0	0.5	2.0	3.0	10.0	18.5	17.0	2.0	**53**	4.06
Open grassland	6.0	0.4	5.0	3.0	15.0	65.0	175.0	25.0	**294**	22.53
Other	0.0	0.5	1.0	0.0	1.0	1.0	48.0	114.0	**165**	12.57
Total (2011)	**76**	**278**	**215**	**19**	**118**	**117**	**319**	**163**	**1304**	n.a.
% of total area	5.90	21.30	16.48	1.38	8.97	8.97	24.45	12.57	n.a.	100

TABLE 3 Error matrix for the land cover map for 2006.[a)]

Land cover	Closed needle-leaved forest	Open needle-leaved forest	Closed shrubland	Open shrubland	Closed grassland	Open grassland	Agriculture	Built-up area	Barren area	River/riverbed	Total	User's accuracy (%)
Closed needle-leaved forest	10	3									13	76.92
Open needle-leaved forest	1	18									19	94.74
Closed shrubland		2	12	1							15	80.00
Open shrubland			1	8							9	88.89
Closed grassland					17	1					18	94.44
Open grassland					1	15	1				17	88.24
Agriculture					1		25				26	96.15
Built-up area								5			5	100.00
Barren area							1		10		11	90.91
River/riverbed										7	7	100.00
Total	11	23	13	9	19	16	27	5	10	7	140	n.a.
Producer's accuracy (%)	90.91	78.26	92.31	88.89	89.47	93.75	92.59	100.00	100.00	100.00	n.a.	n.a.

[a)]Total number of samples = 140; number of accurate samples = 127; overall accuracy = 90.71%; standard error of kappa = 0.02; 95% confidence interval = 0.770 to 0.850; weighted kappa = 0.906; overall user's accuracy = 91.257%; kappa = 0.81; overall producer's accuracy = 92.61%.

http://dx.doi.org/10.1659/MRD-JOURNAL-D-14-00074.1

TABLE 4 Error matrix for the land cover map for 2011.[a)]

Land cover	Closed needle-leaved forest	Open needle-leaved forest	Closed shrubland	Open shrubland	Closed grassland	Open grassland	Agriculture	Built-up area	Barren area	River/riverbed	Total	User's accuracy (%)
Closed needle-leaved forest	**11**	2									13	84.62
Open needle-leaved forest	1	**20**									21	95.24
Closed shrubland			**12**	1							13	92.31
Open shrubland			1	**8**							9	88.89
Closed grassland					**17**	1					18	94.44
Open grassland		1			1	**15**	1				18	83.33
Agriculture							**25**				25	100.00
Built-up area								**5**			5	100.00
Barren area							1		**10**		11	90.91
River/riverbed										**7**	7	100.00
Total	12	23	13	9	18	16	27	5	10	7	**140**	n.a.
Producer's accuracy (%)	91.67	86.96	92.31	88.89	94.44	93.75	92.59	100.00	100.00	100.00	n.a.	n.a.

[a)]Total number of samples = 140; number of accurate samples = 130; overall accuracy = 92.86%; overall user's accuracy = 92.97%; overall producer's accuracy = 94.06%; standard error of kappa = 0.02; 95% confidence interval = 0.770–0.850; weighted kappa = 0.906; kappa = 0.81.

and arable land. Water, fuelwood, and other forest resources are scarce, and their availability is further reduced by the increasing demand from the 3 local communities. Agricultural production relies entirely on irrigation, and the watershed is being increasingly used at unsustainable levels, with overgrazing and overharvesting of fuelwood and timber leading to ecosystem degradation (Paudel 2007).

In remote areas, there may be less awareness among policy-makers of the existence and scale of forest loss and of the long-term implications, because repeated ground-based measurements are intensive and costly and thus virtually nonexistent (Lu 2006). Alternative possibilities for meeting immediate needs for fuelwood and timber are also considerably more limited in remote areas, and even where guidelines or laws exist, possibilities for enforcement are limited (Mather 2007). The area is dominated by rangeland, with only small areas of forest and arable land. Water, fuelwood, and other forest resources are scarce, and their availability is further reduced by the increasing demand from the 3 local communities. Agricultural production relies entirely on irrigation, and the watershed is being increasingly used at unsustainable levels, with overgrazing and overharvesting of fuelwood and timber leading to ecosystem degradation (Mather 2007).

There was some indication that forest management in this area was poor. Participatory appraisal research with the local communities revealed that the current forest governance norms were inadequate, and follow-up by local line agencies on community-based forest operational plans was very limited (Acharya et al 2008). It appeared that timber was being "leaked" out of Jumla district, both legally and illegally. Remoteness, inadequate forest governance, and authorized and unauthorized overuse of local forests in Lorpa have resulted in continuing deforestation and forest degradation (Paudel 2007). LC maps and information derived from satellite images of the type reported here can help increase awareness and understanding of the problems, support the development of appropriate management plans, and provide a low-cost means for detailed monitoring of forest status.

To be low cost, satellite images have to be widely available. However, obtaining appropriate satellite images, free of cloud cover, snow, or other defects from the same source and month in different years for a particular area, can be problematic. In this study, the

http://dx.doi.org/10.1659/MRD-JOURNAL-D-14-00074.1

images available for the different years were from different sources and a different month (QuickBird from 18 November 2006 and IKONOS from 24 October 2011) and had a different spatial resolution (0.5 m for QuickBird and 1 m for IKONOS). However, it is unlikely that these differences had any marked effect on the results. The 3 weeks' difference in the date is unlikely to have had any noticeable effect on the analysis, because the coniferous trees retain their needles, and the visual characteristics of other classes also vary little at this time of year. The difference in resolution is also unlikely to have affected the tree count, because the great majority of trees had a tree crown diameter considerably greater than the limits of resolution (Ke and Quackenbush 2011). This assumption was further supported by the very high level of accuracy determined in the tree counts in the lower-resolution IKONOS image.

Ke and Quackenbush (2011) noted that one problem often encountered with GEOBIA algorithms is off-nadir imagery. Through most of the high-resolution optical stereo images, a high-resolution DEM can be produced for orthorectification. However, these high-resolution DEMs are very costly, so the study used the SRTM DEM with integration of rational polynomial coefficient files (St-Onge et al 2008). Distortion was measured in the QuickBird image using the ground points as a reference. A deviation of 47.37° was detected in the sensor azimuth angle, which can lead to a spatial distortion in the tree comparison. To overcome this problem, the IKONOS image was further rectified geometrically, following orthorectification, using the reference points in the QuickBird image.

There are a number of effects that can cause difficulties in the interpretation of satellite images and detection and delineation of tree crowns. These include the effects of shadow from surrounding hills and mountains, the intermingling of tree crowns, topography, and GPS readings from the field (Dare 2005). In this study, some of these were addressed through manual scanning of the images, followed by geometric correction. Although our algorithm takes advantage of both spectral and spatial information to separate individual trees and to locate treetops, some potential problems deserving further research still exist (Wang et al 2004).

Tree contour detection methods using satellite images are sensitive to noise, or texture, especially in mountainous regions, so preprocessing is essential (Immitzer et al 2012). Blaschke et al (2014) used the term "trivial" in the context of classification where the object has a unique spectral "signature," but in reality it is very difficult to retain a similar spectral response for a particular feature throughout an image. Although VHR satellite images provide very refined objects through segmentation, it is still difficult to extract the range of spectral values for particular LC features (Gilani et al 2015). In this study, a multispectral image (4 bands) with spectral indices and DEM-based derived information were used as a basis for rule-based GEOBIA, which improved detection and delineation of the tree crowns.

Other possibilities apart from optical satellite data are also becoming available to improve detection and delineation of individual tree crowns. Integration of active (LiDAR, radar) and passive satellite data has been shown to produce more effective and efficient tree crown identification (Leckie et al 2003; Ke and Quackenbush 2011). Previously one of the major limitations of VHR satellite data was the limited number of spectral bands (Herold et al 2003), but this has now been overcome with WorldView-2 and similar products. In the future, species-level identification, monitoring, and assessment will be able to provide an effective means of support for improved forest management and associated local decision-making (Immitzer et al 2012).

Conclusion

This study showed that it is possible to use GEOBIA techniques with widely available VHR satellite images (QuickBird and IKONOS) to detect, delineate, and count tree crowns, prepare LC maps, and detect changes in tree number and LC over time, in a cost-effective manner, for the remote mountain valleys of Nepal. The GEOBIA region-growing algorithm provided effective and accurate results on the detection and delineation of tree crowns. The results showed a high level of deforestation (approximately 90 trees per month on average over 5 years), which appeared to be related to poor forest governance and the remoteness of the area. This was somewhat unexpected, as in more accessible areas of the country, deforestation and forest degradation are reported to have been reduced and even reversed in recent years as a result of the successful community forestry program.

Although there were a number of potential sources of error in the results, including orthorectification, incident angle, shadows, topography, and GPS readings, these could be addressed through knowledge of the ground realities and visual interpretation of images. The overall accuracy achieved in this study was extremely high, although monitoring at tree species level remains to be assessed. Thus the methodology provides a low-cost and feasible way to obtain the information needed to raise community awareness and support planning and decision-making for improved forest management in remote and poorly accessible mountain watersheds.

http://dx.doi.org/10.1659/MRD-JOURNAL-D-14-00074.1

ACKNOWLEDGMENTS

We acknowledge the support of the Asian Development Bank (ADB) for the research through funding of the High Mountain Agri-business and Livelihood Improvement (HIMALI) Project (HIMALI). Thanks are due to Renate Fleiner, Govinda Joshi, and Madhav Dhakal for providing extensive field information for validation of results. Our special gratitude goes to Basanta Shrestha, director of strategic cooperation, and Birendra Bajracharya, program manager, at Mountain Environment Regional Information System (MENRIS), for their encouragement and support. We also thank our project partner Local Initiatives for Biodiversity, Research and Development (LI-BIRD) for their constructive and gracious cooperation. Our sincere thanks go to A. Beatrice Murray for language editing of the manuscript.

REFERENCES

Acharya KP, Adhikari J, Khanal D. 2008. Forest tenure regimes and their impact on livelihoods in Nepal. *Journal of Forest and Livelihood* 7(1):6–18.

Agrawal A, Chhatre A. 2006. Explaining success on the commons: Community forest governance in the Indian Himalaya. *World Development* 34(1): 149–166.

Baccini A, Friedl M, Woodcock C, Warbington R. 2004. Forest biomass estimation over regional scales using multisource data. *Geophysical Research Letters* 31:1–4.

Bai Y, Walsworth N, Roddan B, Hill DA, Broersma K, Thompson D. 2005. Quantifying tree cover in the forest-grassland ecotone of British Columbia using crown delineation and pattern detection. *Forest Ecology and Management* 212(1–3):92–100.

Bajracharya B, Uddin K, Chettri N, Shrestha B, Siddiqui SA. 2010. Understanding land cover change using a harmonized classification system in the Himalaya. *Mountain Research and Development* 30(2):143–156.

Blaschke T. 2010. Object based image analysis for remote sensing. *ISPRS Journal of Photogrammetry and Remote Sensing* 65(1):2–16.

Blaschke T, Hay GJ, Kelly M, Lang S, Hofmann P, Addink E, Queiro-Feitosa R, van der Meer F, van der Werff H, van Coillie F, Tiede D. 2014. Geographic object-based image analysis—Towards a new paradigm. *ISPRS Journal of Photogrammetry and Remote Sensing* 87:180–191.

Brandtberg T. 2002. Individual tree-based species classification in high spatial resolution aerial images of forests using fuzzy sets. *Fuzzy Sets and Systems* 132(3):371–387.

Chubey MS, Franklin SE, Wulder MA. 2006. Object-based analysis of IKONOS-2 imagery for extraction of forest inventory parameters. *Photogrammetric Engineering and Remote Sensing* 72:383–394.

Coillie FMB, Verbeke LPC, Wulf RR. 2008. Semi-automated forest stand delineation using wavelet based segmentation of very high resolution optical imagery. *In:* Blaschke T, Lang S, Hay GJ, editors. *Object-Based Image Analysis*. Berlin and Heidelberg, Germany: Springer, pp 237–256.

Cui W, Guan Z, Zhang Z. 2008. An improved region growing algorithm for image segmentation. Paper presented at the International Conference on Computer Science and Software Engineering, Wuhan University, Wuhan, China. Published in Vol 6 of the IEEE proceedings.

Culvenor DS. 2002. TIDA: An algorithm for the delineation of tree crowns in high spatial resolution remotely sensed imagery. *Computers & Geosciences* 28:33–44.

Dare PM. 2005. Shadow analysis in high-resolution satellite imagery of urban areas. *Photogrammetric Engineering & Remote Sensing* 70(2):169–177.

Erdody TL, Moskal LM. 2010. Fusion of LiDAR and imagery for estimating forest canopy fuels. *Remote Sensing of Environment* 114(4):725–737.

Erikson M. 2003. Segmentation of individual tree crowns in colour aerial photographs using region growing supported by fuzzy rules. *Canadian Journal of Forest Research* 33(8):1557–1563.

Erikson M. 2004. Species classification of individually segmented tree crowns in high-resolution aerial images using radiometric and morphologic image measures. *Remote Sensing of Environment* 91:469–477.

Erikson M, Olofsson K. 2005. Comparison of three individual tree crown detection methods. *Machine Vision and Applications* 16(4):258–265.

FAO [Food and Agriculture Organization of the United Nations]. 2011. State of the World's Forests 2011. Rome, Italy: Food and Agriculture Organization of the United Nations.

Foody MG. 2002. Status of land cover classification accuracy assessment. *Remote Sensing of Environment* 80:185–201.

Gibbs HK, Brown S, Niles JO, Foley JA. 2007. Monitoring and estimating tropical forest carbon stocks: Making REDD a reality. *Environmental Research Letters* 2(4):045023.

Gilani H, Shrestha HL, Murthy M, Phuntso P, Pradhan S, Bajracharya B, Shrestha B. 2015. Decadal land cover change dynamics in Bhutan. *Journal of Environmental Management* 148:91–100.

Gilmour D. 1990. Resource availability and indigenous forest management systems in Nepal. *Society & Natural Resources* 3(2):145–158.

Hansen M, DeFries R, Townshend J, Carroll M, Dimiceli C, Sohlberg R. 2003. Global percent tree cover at a spatial resolution of 500 meters: First results of the MODIS vegetation continuous fields algorithm. *Earth Interactions* 7(10):1–15.

Hay GJ, Castilla G, Wulder MA, Ruiz JR. 2005. An automated object-based approach for the multiscale image segmentation of forest scenes. *International Journal of Applied Earth Observation and Geoinformation* 7(4):339–359.

Herold M, Gardner ME, Roberts DA. 2003. Spectral resolution requirements for mapping urban areas. *Geoscience and Remote Sensing* 41(9):1907–1919.

Hussin YA, Gilani H, Leeuwen L, Murthy MSR, Shah R, Baral S, Tsendbazar N-E, Shrestha S, Shah SK, Qamer FM. 2014. Evaluation of object-based image analysis techniques on very high-resolution satellite image for biomass estimation in a watershed of hilly forest of Nepal. *Applied Geomatics* 6(1):59–68.

Immitzer M, Atzberger C, Koukal T. 2012. Tree species classification with random forest using very high spatial resolution 8-band WorldView-2 satellite data. *Remote Sensing* 4:2661–2693.

Karki S, Joshi L, Karky B. 2014. *Learning on Reducing Emissions from Deforestation and Forest Degradation*. Kathmandu, Nepal: International Centre for Integrated Mountain Development.

Ke Y, Quackenbush LJ. 2008. Comparison of individual tree crown detection and delineation methods. Proceedings of the 2008 American Society for Photogrammetry and Remote Sensing (ASPRS) annual conference. Bethesda, MD: ASPRS, no page numbers.

Ke Y, Quackenbush LJ. 2011. A comparison of three methods for automatic tree crown detection and delineation from high spatial resolution imagery. *International Journal of Remote Sensing* 32(13):3625–3647.

Kim M, Madden M, Warner TA. 2009. Forest type mapping using object-specific texture measures from multispectral Ikonos imagery: Segmentation quality and image classification issues. *Photogrammetric Engineering and Remote Sensing* 75(7):819–829.

Kim SR, Kwak DA, Lee WK, Son Y, Bae SW, Kim C, Yoo S. 2010. Estimation of carbon storage based on individual tree detection in *Pinus densiflora* stands using a fusion of aerial photography and LiDAR data. *Science China Life Sciences* 53(7):885–897.

Knorn J, Rabe A, Radeloff VC, Kuemmerle T, Kozak J, Hostert P. 2009. Land cover mapping of large areas using chain classification of neighboring Landsat satellite images. *Remote Sensing of Environment* 113(5):957–964.

Lambin EF, Meyfroidt P. 2011. Global land use change, economic globalization, and the looming land scarcity. *Proceedings of the National Academy of Sciences* 108(9):3465–3472.

Larsen M, Eriksson M, Descombes X, Perrin G, Brandtberg T, Gougeon FA. 2011. Comparison of six individual tree crown detection algorithms evaluated under varying forest conditions. *International Journal of Remote Sensing* 32(20):5827–5852.

Latif ZA, Zamri I, Omar H. 2012. Determination of tree species using Worldview-2 data. Paper presented at the 2012 IEEE 8th International Colloquium on Signal Processing and its Applications, 23–25 March, Melaka, Malaysia.

Leboeuf A, Beaudoin A, Fournier R, Guindon L, Luther J, Lambert M. 2007. A shadow fraction method for mapping biomass of northern boreal black spruce forests using QuickBird imagery. *Remote Sensing of Environment* 110(4): 488–500.

Leckie DG, Gougeon FA, Walsworth N, Paradine D. 2003. Stand delineation and composition estimation using semi-automated individual tree crown analysis. *Remote Sensing of Environment* (85):355–369.

Lévesque J, King DJ. 2003. Spatial analysis of radiometric fractions from high-resolution multispectral imagery for modelling individual tree crown and forest canopy structure and health. *Remote Sensing of Environment* 84(4):589–602.

Lu D. 2006. The potential and challenge of remote sensing based biomass estimation. *International Journal of Remote Sensing* 27(7):1297–1328.

Mather AS. 2007. Recent Asian forest transitions in relation to forest-transition theory. *International Forestry Review* 9(1):491–502.
Mathieu R, Aryal J, Chong AK. 2007. Object-based classification of IKONOS imagery for mapping large-scale vegetation communities in urban areas. *Sensors* 7:2860–2880.
Mbaabu P, Hussin Y, Weir M, Gilani H. 2014. Quantification of carbon stock to understand two different forest management regimes in Kayar Khola watershed, Chitwan, Nepal. *Journal of the Indian Society of Remote Sensing* 42(4):745–754.
Mora B, Wulder MA, White JC. 2010. Segment-constrained regression tree estimation of forest stand height from very high spatial resolution panchromatic imagery over a boreal environment. *Remote Sensing of Environment* 114(11): 2474–2484.
National Population and Housing Census. 2012. *National Population and Housing Census 2011*. Kathmandu, Nepal: Government of Nepal National Planning Commission Secretariat, Central Bureau of Statistics.
Niraula RR, Gilani H, Pokharel BK, Qamer FM. 2013. Measuring impacts of community forestry program through repeat photography and satellite remote sensing in the Dolakha district of Nepal. *Journal of Environmental Management* 126:20–29.
Olofsson K, Wallerman J, Holmgren J, Olsson H. 2006. Tree species discrimination using Z/I DMC imagery and template matching of single trees. *Scandinavian Journal of Forest Research* 21:106–110.
Olofsson P, Foody GM, Stehman SV, Woodcock CE. 2013. Making better use of accuracy data in land change studies: Estimating accuracy and area and quantifying uncertainty using stratified estimation. *Remote Sensing of Environment* 129:122–131.
Paudel M. 2007. Non-timber forest products from community forestry practices, problems and prospects for livelihood strategy in Jumla. *Banko Janakari* 17(2): 45–54.
Platt RV, Schoennagel T. 2009. An object-oriented approach to assessing changes in tree cover in the Colorado Front Range 1938–1999. *Forest Ecology and Management* 258(7):1342–1349.
Potere D. 2008. Horizontal positional accuracy of Google Earth's high-resolution imagery archive. *Sensors* 8(12):7973–7981.
Pouliot DA, King DJ, Bell FW, Pitt DG. 2002. Automated tree crown detection and delineation in high-resolution digital camera imagery of coniferous forest regeneration. *Remote Sensing of Environment* 82(2–3):322–334.
Pu R, Landry S. 2012. A comparative analysis of high spatial resolution IKONOS and WorldView-2 imagery for mapping urban tree species. *Remote Sensing of Environment* 124:516–533.
Pu R, Landry S, Yu Q. 2011. Object-based urban detailed land cover classification with high spatial resolution IKONOS imagery. *International Journal of Remote Sensing* 32(12):3285–3308.
Qamer F, Abbas S, Saleem R, Shehzad K, Ali H, Gilani H. 2012. Forest cover change assessment in conflict-affected areas of northwest Pakistan: The case of Swat and Shangla districts. *Journal of Mountain Science* 9(3):297–306.
Quintano C, Cuesta E. 2010. Improving satellite image classification by using fractional type convolution filtering. *International Journal of Applied Earth Observation and Geoinformation* 12(4):298–301.
Shih FY, Cheng S. 2005. Automatic seeded region growing for color image segmentation. *Image and Vision Computing* 23(10):877–886.
Smith K. 2013. Environmental Hazards: Assessing Risk and Reducing Disaster. New York, NY: Routledge.
St-Onge B, Hu Y, Vega C. 2008. Mapping the height and above ground biomass of a mixed forest using lidar and stereo Ikonos images. *International Journal of Remote Sensing* 29(5):1277–1294.
Stathakis D, Vasilakos A. 2006. Satellite image classification using granular neural networks. *International Journal of Remote Sensing* 27(18):3991–4003.
Stehman SV, Czaplewski RL. 1998. Design and analysis for thematic map accuracy assessment: Fundamental principles. *Remote Sensing of Environment* 64:331–344.
Suwandana E, Kawamura K, Sakuno Y, Kustiyanto E, Raharjo B. 2012. Evaluation of ASTER GDEM2 in comparison with GDEM1, SRTM DEM and topographic-map-derived DEM using inundation area analysis and RTK-dGPS data. *Remote Sensing* 4(8):2419–2431.
Thapa R, Watanabe M, Motohka T, Shiraishi T, Shimada M. 2014. Calibration of aboveground forest carbon stock models for major tropical forests in central Sumatra using airborne LiDAR and field measurement data. *IEEE Journal of Selected Topics in Applied Earth Observations and Remote Sensing* 8(2): 661–673.
Thessler S, Sesnie S, Ramos Bendaña ZS, Ruokolainen K, Tomppo E, Finegan B. 2008. Using k-nn and discriminant analyses to classify rain forest types in a Landsat TM image over northern Costa Rica. *Remote Sensing of Environment* 112(5):2485–2494.
Tiede D, Lang S, Hoffmann C. 2006. Supervised and forest type-specific multi-scale segmentation for a one-level-representation of single trees. *In:* Lang S, Blaschke T, Schöpfer E, editors. *1st International Archives of Photogrammetry, Remote Sensing and Spatial Information Sciences (ISPRS).* Salzburg, Austria: ISPRS, no page numbers.
Tiede D, Lang S, Maier B. 2007. Transferability of a tree-crown delineation approach using region-specific segmentation. *In:* Neves Epiphanio JC, Soares Galvão L, editors. *Anais XIII Simpósio Brasileiro de Sensoriamento Remoto, Florianópolis, Brasil—Brazilian Remote Sensing Symposium*. São José dos Campos, Brazil: Instituto Nacional de Pesquisas Espaciais [INPE], pp 1883–1890.
Tiwari KP. 2010. Agricultural policy review for coffee promotion in Nepal. *Journal of Agriculture and Environment* 11:138–147.
Uddin K, Shrestha HL, Murthy M, Bajracharya B, Shrestha B, Gilani H, Pradhan S, Dangol B. 2015. Development of 2010 national land cover database for the Nepal. Journal of Environmental Management 148:82–90.
Wang L, Gong P, Biging G. 2004. Individual tree crown delineation and treetop detection in high spatial resolution aerial imagery. *Photogrammetric Engineering and Remote Sensing* 70(3):351–357.
Zhou J, Proisy C, Descombes X, le Maire G, Nouvellon Y, Stape J-L, Viennois G, Zerubia J, Couteron P. 2013. Mapping local density of young eucalyptus plantations by individual tree detection in high spatial resolution satellite images. *Forest Ecology and Management* 301:129–141.

Supplemental material

FIGURE S1 Change in tree crown area (based on analysis of QuickBird for 2006 and IKONOS for 2011).
FIGURE S2 Validation of detected and manually delineated trees: (A) for QuickBird 2006; (B) for IKONOS 2011.
FIGURE S3 Land cover changes between 2006 and 2011. Typical areas showing loss of forest cover in the northern part of the watershed; the 2 Quickbird images on the left show 2 sample areas in 2006; the 2 IKONOS images on the right show the same sample areas in 2011.

All found at DOI: 10.1659/MRD-JOURNAL-D-14-00074.S1 (491 KB PDF).